HHS Public Access

Author manuscript

Nanomedicine. Author manuscript; available in PMC 2020 August 01.

Published in final edited form as:

Nanomedicine. 2019 August ; 20: 102009. doi:10.1016/j.nano.2019.04.012.

Anti-biofilm activity of garlic extract loaded nanoparticles

Vallerinteavide Mavelli Girish, PhD[a], **Hongying Liang, PhD**[a], **Jennifer T. Aguilan, PhD**[b,c], **Joshua D. Nosanchuk, MD**[d], **Joel M. Friedman, MD, PhD**[a], **Parimala Nacharaju, PhD**[a]

[a]Department of Physiology and Biophysics, Albert Einstein College of medicine, Bronx, NY 10461

[b]Department of Pathology, Albert Einstein College of medicine, Bronx, NY 10461

[c]Laboratory for Macromolecular Analysis & Proteomics, Albert Einstein College of Medicine, Bronx, NY 10461

[d]Departments of Medicine and Microbiology and Immunology, Albert Einstein College of Medicine, Bronx, NY 10461.

Abstract

The emergence and widespread distribution of multi-drug resistant bacteria is considered as a major public health concern. The inabilities to curb severe infections due to antibiotic resistance have increased healthcare costs as well as patient morbidity and mortality. Bacterial biofilms formed by drug-resistant bacteria add additional challenges to treatment. This study describes a sol-gel based nanoparticle system loaded with garlic extract (GE-np) that exhibits: i) slow and sustained release of garlic components; ii) stabilization of the active components; and iii) significant enhancement of antimicrobial and antibiofilm activity relative to the free garlic extract. Also, GE-np were efficient in penetrating and disrupting the well-established methicillin-resistant *Staphylococcus aureus* (MRSA) biofilms. Overall, the study suggests that GE-np might be a promising candidate for the treatment of chronic infections due to biofilm forming drug-resistant bacteria.

Graphical Abstract

Representative 3D images showing anti-biofilm effect of garlic extract loaded nanoparticles (GE-np) and its comparison to equivalent garlic extract (eqGE), mupirocin, blank nanoparticles (blank-np) and medium alone (untreated) on well-established MRSA biofilms. The biofilms were stained using bacterial viability kit [live (green) and dead (red/yellow)]. The scale bars represent 100 μm for all images.

Correspondence: Parimala Nacharaju, Department of Physiology and Biophysics, Albert Einstein College of medicine, 1300 Morris Park Avenue, Bronx, NY 10461 Tel: +1-718-430-8571 (Office); fax: +1-718-430-8819, pnacharaju@gmail.com, parimala.nacharaju@einstein.yu.edu.

Conflict of interest:
None of the authors have any conflict of interest to declare.

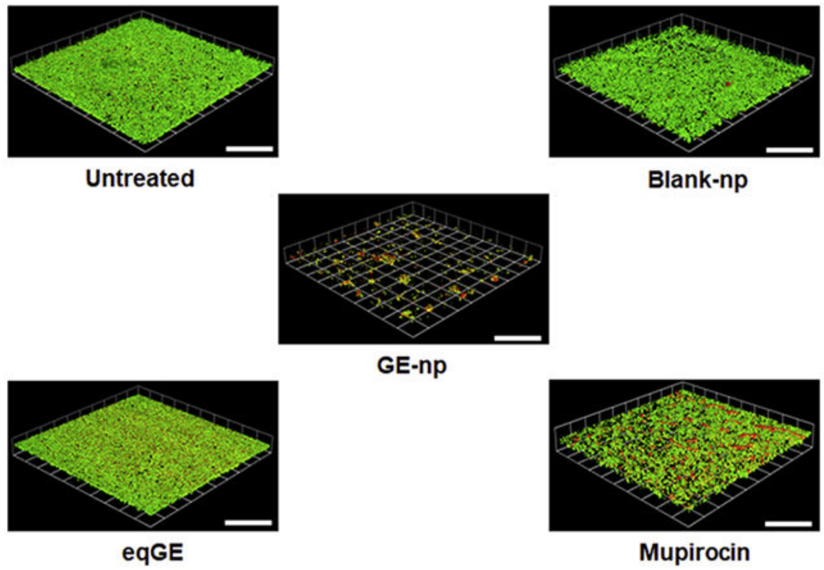

Keywords

Garlic extract; nanoparticles; MRSA; biofilm; antibacterial

Background:

A biofilm is an assembly of surface-associated microbial cells enclosed in an extracellular polymeric substance that is primarily a polysaccharide matrix, secreted by microbial cells. Biofilms may form on a wide variety of surfaces, including living tissues, indwelling medical devices, industrial or potable water system piping, or natural aquatic systems. [1] Bacteria, such as *Staphylococcus aureus, Escherichia coli*, and *Pseudomonas aeruginosa*, and fungi, such as *Candida albicans*, are well known for forming biofilms. [1,2] Planktonic bacteria (freely suspended single cell bacteria) or clusters of cells released from biofilms spread into the bloodstream potentially causing serious consequences. [1] Extracellular polymeric substances (EPS) in biofilms reduce the penetration of host immune agents as well as antimicrobials and give rise to extreme therapeutic recalcitrance (i.e. enhancing the microbe’s ability to survive in the presence of high serum and/or tissue concentrations of antibiotics) thus posing serious treatment challenges for many persistent biofilms and associated infections. [1]

Lung infections in cystic fibrosis, chronic forms of urinary tract infection (UTI), sinusitis, tonsillitis, and biliary tract infection are some examples for host tissue associated biofilm infections. Implant-biofilm related infections are often associated with orthopedic implants (bone, hip and knee replacements), root canal, vascular and urinary catheters, pace makers etc. [1,3,4] The non-vascular nature of the implants impairs the access of immune system cells to the surrounding area of the implants. [3, 5] Therefore, patients with such implants are especially vulnerable to chronic infections. In most cases, antimicrobial therapy combined with the removal of the colonized device or surgical excision of infected tissue is the only efficient way to eradicate a biofilm-related infection. [4]

Current anti-biofilm approaches include systemic antibiotic prophylaxis during device insertion, antibiotic coating of implanted devices before insertion, early removal of an unnecessary device, surgical removal of biofilm and optimization of the antibiotic regimen against biofilm induced infections. [1,3,4] In addition to the choice of specific antibiotics, high dosages and prolonged treatment courses are required for biofilm-associated infections. Such chronic treatment with antibiotics can lead to drug resistance of bacteria and an increased risk for drug toxicities. Therefore, the search for new and more effective therapeutics is warranted.

Natural product based therapeutics are gaining significant attention recently both for their antimicrobial efficiency and for not inducing drug resistance. Garlic, chitosan derivatives, various spices and antimicrobial peptides are examples for such products. [6-9] Garlic (*Allium sativum*) is well known for its antimicrobial activity against different types of bacteria, viruses and fungi. [10-12] Organosulfur compounds present in garlic are responsible for its antimicrobial activity. The major component, allicin is proposed to exert its antimicrobial activity through multiple mechanisms. Antimicrobial agents acting through multiple mechanisms may induce little or no resistance to microorganisms. [13] The proposed mechanisms for antimicrobial activity of allicin, a major component of garlic, include its 1) membrane permeable capability and ability to destroy cell structure, [14,15] 2) ability to alter gene expression of microorganisms, [14] 3) reactivity with thiol containing enzymes thereby inducing oxidative stress. [16,17]

The extracellular matrix surrounding and released by bacteria is mostly responsible for biofilm recalcitrance. Many studies suggest that mechanical and physicochemical properties of the biofilm, electrical interactions and charge compatibility of the therapeutics and biofilm matrices influence the outcome of a treatment. [18-20] The extracellular matrix is different for different biofilms and therefore necessitates the use of compatible antimicrobial agents to penetrate the specific biofilms. [1] Additionally, an antimicrobial agent capable of penetrating a biofilm matrix may not be efficient at destroying the microorganism. Similarly, an agent with good activity against a microorganism may not be able to penetrate into its biofilm matrix. Some antibiotics capable of penetrating into biofilms do not eradicate 100% of biofilm bacteria. In this regard, a delivery system that can both penetrate most or all biofilms and deliver any of a large number of different organism specific or broad-spectrum antimicrobial agents would be extremely beneficial with broad applicability for diverse indications.

We have developed a sol-gel based nanoparticle system capable of penetrating biofilms and delivering virtually any non-protein based therapeutic agent. The advantages of sol-gel nanoparticle system are 1) particle size, surface charge and hydrophobicity can be manipulated, which may allow penetration into different biofilms, 2) any small to medium sized antimicrobial agents can be loaded, and 3) slow release of the loaded antimicrobial agents that allows for drug delivery within inner layers of biofilm.

We chose garlic components as a highly promising antimicrobial agent to load in our nanoparticles to test against biofilms. Our preliminary studies with the total garlic extract

(GE) loaded in sol-gel nanoparticles (garlic extract-np or GE-np) show excellent anti-biofilm activity against MRSA in vitro.

Methods:

Preparation of sol-gel:

The sol-gel was prepared with tetramethylorthosilicate (TMOS; Sigma-Aldrich, St. Louis, MO) as described by Brinker et al with minor modifications. [21] Briefly, two aliquots of 3 ml TMOS were hydrolyzed separately by 0.37 ml of 40 mM HCl in the presence of 2.5 ml MeOH at 60 °C for 1.5 h. One aliquot was diluted with 1.152 ml water and incubated at 40 °C for polymerization. It formed a clear gel in 72 h. The second aliquot was diluted with 1.152 ml water and 20 μl of similarly hydrolyzed 3-aminopropyltrimethosysilane (APTS; Gelest Inc. Morrisville, PA) was added. Since most of the antimicrobial components of GE are organosulfur compounds, we expected APTS to induce more sustained release of these components from the sol-gel nanoparticles. The polymerization of this mixture was carried out at 40 °C. It formed a clear gel in 24 h.

Preparation of garlic extract loaded nanoparticles:

About 2 g of gel was mashed with a glass rod followed by the addition of 2 ml of 20% ethanol and cooling on ice. To this gel, 2 ml of 4x diluted total GE (see Supplementary Material for the preparation of GE) was added and mixed on a mini-lab roller (Labnet International, Edison, NJ) overnight at 4 °C. The mixture was centrifuged at 1900 g for 4 min, supernatant separated and particles lyophilized. The dried powder was ground into finer particles in mortar-pestle to give the final products, GE-np-control (without APTS) and GE-np (with APTS), and stored in aliquots at −80 °C. The concentration of total GE in nanoparticles was expressed in terms of allicin content, a major component of the extract.

Rate of release of garlic components from GE-np and stability of allicin:

GE-np-control and GE-np were dispersed in PBS at 5 mg/ml and mixed on a mini-lab roller at room temperature. At time intervals, aliquots were drawn, centrifuged at 17,000 g. The supernatants were separated and the absorption at 210 nm of the extract was recorded on a spectrophotometer (Thermo Fisher Scientific, Waltham, MA). To determine the stability of allicin in the extracts, GE-np was dispersed in PBS at 2.5 mg/ml at 37 °C. GE at equivalent concentration was taken in PBS at the same temperature. At time intervals, aliquots taken out from both GE-np and GE samples were processed and analyzed on reverse-phase HPLC (RP-HPLC) as described in the supplementary material. The amount of allicin present in aliquots was calculated from the allicin peak area.

Antibacterial effect of GE-np:

The susceptibility of MRSA strain 6524 (for details see Supplementary Material) to GE-np was evaluated through a colony forming unit (CFU) count assay. An overnight grown culture of MRSA in TSB was diluted to 10^8 cells ml^{-1} based on McFarland equivalence turbidity standard 0.5 (Thermo Fisher Scientific, Waltham, MA). The bacterial suspension was then adjusted to 10^5 cells ml^{-1} in TSB, treated with varying concentrations of GE-np (0.625, 1.25, 2.5 or 5 mg/ml) or GE at the equivalent concentrations (eqGE) or blank nanoparticles (blank-np) at 5 mg/ml. Untreated bacteria served as control for this experiment. The suspension was constantly mixed using a tube rotator (Bellco Glass Inc, Vineland, NJ) to ensure uniform distribution and incubated at 37 °C for 6 h. After the incubation, different dilutions of the suspension in PBS were plated on tryptic soy agar (TSA; MP Biomedicals, Santa Ana, CA). The bacterial viability was assessed by counting the number of colonies established on the agar plate after overnight incubation at 37 °C. CFUs were normalized by considering the untreated bacterial cells as 100% of bacterial viability. All experiments were conducted in triplicates at three independent trials.

Anti-biofilm effect of GE-np:

The ability of GE-np to disrupt the bacterial biofilm and reduce the viable cells was evaluated according to the method of Jurcisek et al with minor modifications. [22] Briefly, 500 μl of a standardized log-phase MRSA suspension (10^8 cells ml$-^1$) was seeded into each well of a Nunc™ Lab-Tek™ 8-well chambered cover glass system (Thermo Fisher Scientific, Waltham, MA) and incubated for 48 h at 37 °C without shaking. The media was changed after 24 h to maintain the bacterial viability. After 48 h, the media was aspirated and the wells were washed twice with sterile PBS to remove any non-adhered bacteria. The biofilms were then treated with either GE-np (5 mg/ml) or eqGE or blank-np. Mupirocin (Sigma-Aldrich, St. Louis, MO) at 1 mg/ml was used as the positive control. Untreated wells were used as negative control. All the treatments were done in TSB and the chamber system was incubated for 6 h at 37 °C. The wells were then aspirated and washed twice with sterile PBS. To evaluate the viability of bacterial cells, the wells were treated with BacLight Live/Dead stain (Ex: 488 nm/Em: 500 and 635 nm; Thermo Fisher Scientific, Waltham, MA) based on the manufactures protocol. The biofilm architecture was analyzed using concanavalin A alexa fluor 488 conjugate (Ex: 488 nm/Em: 520 nm) and FilmTracer SYRO ruby biofilm matrix stain (Ex: 458 nm/Em: 610 nm); Thermo Fisher Scientific, Waltham, MA. All the staining was done for 45 min at room temperature, followed by fixing with 10% buffered formalin for 20 min. After a final PBS wash, the microscopic analysis of the biofilm was carried out in a Leica SP5 confocal scanning laser microscope using a 63X oil immersion objective. The images were acquired with 1024 X 1024 resolutions in at least 10 different regions of each surface analyzed. Regions on biofilm with similar depth/thickness were considered for the analysis. The images captured were quantitatively analyzed using Volocity software v6.3 (PerkinElmer, Houston, TX).

In order to determine the penetration/diffusion of nanoparticles into biofilms, blank-np was labeled with SYTO9 dye. Blank-np was treated with SYTO9 dye for 4 h followed by washing with PBS to remove unbound dye. These particles are applied to 48 h grown biofilms. The experimental details are the same as mentioned above, except that the biofilms are stained by concanavalin A 405 conjugate (Ex: 405 nm/Em: 431 nm; Biotium, Fremont, CA), specific for the polysaccharide component of the EPS. All the experiments were done in two independent occasions.

XTT reduction assay:

The total metabolic activity of biofilm cells was measured through XTT assay as described. [23] The biofilm was grown in a 96-well microtiter polystyrene plate as above. After the PBS wash, multiple wells were treated with GE-np at 5 mg/ml or its eqGE or blank-np at 5 mg/ml. Mupirocin at 1 mg/ml and untreated wells were considered as positive and negative controls, respectively. The plates were incubated for 6 h at 37 °C. Post wash, the wells were incubated with a freshly prepared mixture of 0.25 mg/ml XTT and 0.3 mg/ml phenazine methosulfate (Sigma-Aldrich, St. Louis, MO) for 30 min at 37 °C in the dark. A 100 μl aliquot of the resulting colored solution was transferred to the wells of a new 96-well microtiter plate. The absorbance was read at 492 nm in a microplate reader. All the experiments were performed in three independent assays.

Statistical analysis:

All experiments were performed at least in three independent sets and data was represented as mean ± SD. All graphical evaluations were made using GraphPad Prism 7.0 (GraphPad Software Inc., La Jolla, CA). Analysis of variance (ANOVA) was used to evaluate the significant differences and $p<0.05$ was considered significant.

Results:

Characterization of allicin in the garlic extract:

Since allicin is the major antimicrobial component of our extracts and thus the nanoparticles, we characterized and quantified it in the GE prepared. Figure 1 shows the components of the GE eluted into several peaks. The major peak, well separated from other peaks, overlapped with allicin peak from the standard. A pool of fractions from this peak was subjected to ESI-MS (data not shown) and ESI-MS/MS analysis (for detailed methodology see Supplementary Material) together with the allicin standard (Figure 2). The fragmentation pattern of both the samples in MS/MS analysis very well matched, confirming the identity of allicin in the GE. Accordingly, the amount of allicin was quantified from the peak area by comparing it with that of known amount of the standard. The allicin concentration in the GE was determined to be 4.2 mg/ml.

Rate of release of garlic extract from GE-np:

The release rate of garlic components from GE-np in PBS was studied at room temperature. The contents of GE-np-control were released almost immediately after dispersing into PBS. In contrast, GE-np exhibited a sustained release of the garlic components. After an initial burst, a slow release of the contents was observed thereafter (Figure 3A). The initial rapid release may be due to the release from the surface of the nanoparticles, and the contents contained within the particles are released at a slower rate. Some electrostatic interactions between APTS and organosulfur compounds of garlic extract seem to contribute to the sustained release of these products. Since GE-np exhibited a better release rate of garlic products than GE-np-control, GE-np were used for further studies. The RP-HPLC chromatograms of the aliquots didn't show any significant differences in terms of individual peak ratios at different time intervals (data not shown) indicating that all the garlic components are released at the same rate. This also indicates that all the components are stable at room temperature at the time span studied. Therefore, it is justified to use allicin concentration to represent the total GE concentration in the GE-np. The allicin concentration in GE-np was determined to be 2 μg/mg of nanoparticles.

We determined the degradation of allicin, as a representative of the active components of garlic extract, over time at 37 °C. Unlike at room temperature (25 °C), allicin in GE degraded more than 30% in 6 h at 37 °C (Figure 3B). However, allicin in GE-np degraded less rapidly than in GE. Slow release of the active components from GE-np seems to protect them. Thus, this sol-gel nanoparticle system not only provides antimicrobial components of garlic extract at a sustained rate but also protects them from degradation.

Antibacterial properties of GE-np:

The dose-dependent effect of GE-np on the growth of planktonic form of MRSA for up to 6h was studied in detail. GE-np at concentrations of 1.25 mg/ml and above exhibited significant growth inhibition when compared to untreated and blank-np (5 mg/ml). Both GE-np at 5 mg/ml and its eqGE completely inhibited any visible growth of MRSA. However, at lower dilutions, GE-np exhibited higher growth inhibition when compared to the GE. At 2.5 mg/ml and 1.25 mg/ml, GE-np exhibited > 40-folds and ~ 1-fold inhibition, respectively. Blank-np at 5 mg/ml did not affect the growth of bacteria (Figure 4). Taken together, these results suggest that GE-np is effective in significantly reducing the bacterial load when compared to GE.

Anti-biofilm properties of GE-np:

The anti-biofilm efficacy of GE-np was evaluated using a MRSA biofilm cultivated for 48h and this was compared with mupirocin, GE and blank-np. Two different staining procedures were adopted to visualize and quantify biofilm associated cells and the EPS. MRSA biofilms treated with Live/Dead stain showed both live (green) and dead (red) cells. Also, we observed a sub-population of dead cells in yellow (both green and red dye were retained within the cells) especially with GE-np, mupirocin and GE treatment. [24] The EPS is primarily composed of polysaccharides along with proteins and nucleic acids. [25] A combination of concanavalin A-488 and SYPRO ruby was used to stain the polysaccharide (green) and protein (red) components of the EPS, respectively. The MRSA biofilms grown in the absence of any treatment exhibited a homogenous distribution of viable bacterial cells and EPS (Figure 5A, F). The EPS was intact with a measured mean thickness of 9.6 µm (Figure 6A). Biofilms treated with blank-np (Figure 5B, G) demonstrated a comparable morphology and biomass to the untreated ones. However, GE-np, at 5 mg/ml effectively killed the biofilm bacteria with >80% reduction in the viability as well as significantly reduced the biomass (Figure 5C, H). The biofilm architecture was disintegrated with fewer EPS clusters and a mean thickness of 2.3 µm. Also, the volume of biofilm mass with respect to live cells was reduced by 89% (Figure 6). Contrarily, an equivalent amount of GE and mupirocin (1 mg/ml) exhibited lower anti-biofilm activity (~30-40% cell death) with the biofilm thickness comparable to the untreated (Figures 5D, E, I, J and 6). Between GE and mupirocin, mupirocin exhibited 1.5 times higher reduction in biofilm viability (Figure 6).

Discussion:

MRSA is a major cause for nosocomial infections worldwide showing resistance to many of the commonly used antibiotics. [26] Moreover, MRSA is frequently community-acquired. [27] It is one of the 'superbugs' recently listed by WHO as one of the greatest threats to human health. The resulting prolonged, complex illnesses due to MRSA infections have increased the cost of healthcare and contributed to excess morbidity and mortality in diverse patient populations. [28] MRSA has the ability to form biofilms on various physiological surfaces, such as in the lungs of patients with cystic fibrosis, [29] chronic wounds,[30] in the middle ear of patients with chronic otitis media [31] and on the bones and mucosal surface of patients with osteomyelitis and rhinosinusitis, respectively. [32,33] They also colonize various medical implants and catheters and have been observed in many prosthesis-related infections that are very difficult to diagnose and treat[4]. Once established, they are resistant to existing antimicrobial treatments and host immune cells and, hence, enhance the virulence of the infection.

In the present study, we investigated the antibacterial effect of GE-np followed by its potential in disrupting the well-established bacterial biofilms. GE-np was prepared from GE using sol-gel technology, which uniquely allows for the facile manipulation of properties that can accommodate the loading and sustained release of complex deliverables such as garlic extract as well as surface modifications to adhere to different tissue types or medically relevant surfaces. Furthermore, these platforms are highly biocompatible and hydrolytically degraded into water soluble silicic acid, which is both renally excreted and absorbed by the human body. [34,35] Composition analysis of the freshly prepared GE indicated allicin as the principal compound, which agrees with previous studies. [36] At first, we looked at the effect of GE-np on planktonic form of MRSA. The anti-staphylococcal activity, at lower doses of GE-np (1.25 and 2.5 mg/ml) was found to be superior when compared to its eqGE, as shown in Figure 4. This could be because GE-np exhibit a biphasic release profile for GE components with an initial burst release up to 30 min, followed by a slow and extended release over a period of 4 h (Figure 3A) resulting in a prolonged antibacterial effect. Such slow release of GE components also slowdown the degradation of these components as shown for allicin (Figure 3B). Similar observations of enhanced bioavailability and prolonged effect of the drug loaded nanoparticles were previously reported. [37,38] Also, the absence of any EPS on the planktonic MRSA cells could make them more susceptible and vulnerable to the antimicrobial effects of GE-np. [39]

With the growing awareness of bacterial biofilms playing a significant role in antibiotic resistance and other life-threatening medical conditions, we studied the effects of GE-np on a matured MRSA biofilm. We analyzed the bacterial viability without disrupting the biofilm using two robust techniques: Live/Dead BacLight staining that gave a visual representation of live and dead cells based on the membrane integrity and the XTT assay that quantified metabolically active cells. The simultaneous staining of polysaccharides and protein components within the EPS has also enabled us to understand the biofilm integrity. GE-np not only killed MRSA more than 80% at the concentration studied but also destroyed ~98% of the biofilm. Such activity was not observed with GE and the anti-staphylococcal antibiotic, mupirocin. The lower anti-biofilm activity of GE compared to GE-np can be due to multiple factors, including the degradation of active components as well as diffusion of the components into the biofilm. As discussed earlier, allicin in GE degraded more rapidly than in GE-np (Figure 3B). The slow release of the active components seems to slow down the degradation of the components. This may be a major reason for the higher activity of GE-np towards planktonic as well as biofilm associated MRSA. The anti-biofilm potential of mupirocin against MRSA biofilms was evaluated at various concentrations. However, only 1 mg/ml mupirocin and not lesser doses (100 or 10 μg/ml, unpublished observations) exhibited anti-biofilm activity. In fact, this was significantly lower compared to the 5 mg/ml GE-np used, considering a total GE concentration in micrograms per mg of nanoparticles (Figure 6). The poor anti-biofilm activity of mupirocin could be attributed to its low penetrability into biofilms through the EPS. Although mupirocin is a commonly used antibiotic, it's clinical application could be limited with accounts of antimicrobial resistance observed in multiple strains of MRSA. Most recently, it was shown that sub-inhibitory concentrations of mupirocin stimulate biofilm formation in MRSA. [40] These raises the possibility of specific interaction of GE-np with MRSA biofilm. Indeed, our studies with dye labeled blank-np indicated attachment and diffusion of particles into the biofilm matrix (Figure 7). Thus, our sol-gel nanoparticle system not only slow downed the degradation of garlic components but also exposed these components to the inner layers of biofilm and enhanced the effect.

The physico-chemical properties of both the nanoparticles (eg. particle size, charge and surface chemistry) as well as the biofilm (eg. embedded cell density, viscosity, charge and porosity of the EPS) collectively impact their interactions. The functional group moieties on the highly heterogeneous EPS differ in their ability to bind various charged entities like nanoparticles. It is with these differential binding affinities, that nanoparticles initially adhere and accumulate on the biofilm matrix. [41,42] Also, electrostatic or hydrophobic forces could be implicated for the deposition of nanoparticles on the biofilm matrix. [43,44] Subsequently, the nanoparticles driven by diffusion can penetrate through and move within the EPS matrix. [45] Thus, a complete disruption of the biofilm requires efficient adherence and penetration by nanoparticles and subsequent accumulation of the loaded antimicrobials within the biofilm network. Our sol-gel nanoparticles can be modulated in terms of charge and size, which can make them compatible for biofilms of different microbes. The synthetic methods can also be altered for loading of various therapeutic molecules as well as controlling their release rates. Thus, this sol-gel system carries wide applications for indications requiring systemic, topical and transdermal delivery of many therapeutics. The formulation of this sol-gel delivery system is different from the one we have previously formulated. [46] In the previous system, the therapeutic molecules were incorporated into the sol-gel during polymerization step. Therefore, gels needed to be synthesized separately for each therapeutic molecule. [47,48] In the present formulation, a blank gel is prepared first and then loaded with garlic extract. This method is more advantageous than the previous one since a blank gel can be loaded with any therapeutics.

Previous studies have shown the effect of various garlic preparations, either fresh GE or individual components on the bacterial biofilms. [49,50] As described elsewhere, allicin and ajoene in the GE interfere with bacterial biofilm formation through multiple mechanisms. Allicin inhibited the synthesis of polysaccharide intercellular adhesin (PIA), one of the several bacterial adhesins required for biofilm formation in *S. epidermidis*. [51] In *P. aeruginosa* biofilm formation, allicin dramatically reduced the bacterial adhesion and EPS secretion. Moreover, allicin significantly downregulated the expression of various virulence factors like exotoxin A, elastase, rhamnolipids and others involved in quorum sensing (QS). [52] Ajoene, another QS inhibitor is known to downregulate *rhlA* gene expression in *P. aeruginosa* involved in bacterial rhamnolipid synthesis. By this, it prevents the lysis of polymorphonuclear leukocytes, thereby enhancing the host immunity against bacterial infections. Transcriptomic studies have revealed a direct relationship between ajoene concentration and QS gene silencing in *P. aeruginosa*. Among the genes significantly downregulated by ajoene were QS regulated important virulence factors such as chitinase, cytotoxic lectin, chitin binding protein and others. [53] Moreover, ajoene also downregulated the expression of small regulatory RNA molecules in both *P. aeruginosa* and *S. aureus* involved in the production of key QS virulence factors. In *S. aureus*, repression of RNAIII led to the low expression of virulence factors like hemolysins, lipases and various serine and cysteine proteases. [54] Therefore, a QS deficient biofilm can be more fragile to anti-biofilm treatments. Thus, the inhibitory effects of our GE-np to MRSA biofilms could be due to a collective effect of garlic components released from the particles.

Currently, implant-related infections are of great concern since the use of surgically implanted devices has increased to maintain better health. These infections are larger in elderly and the number is increasing due to increased life expectancy. [55] One of the current anti-biofilm strategies includes the prevention of adherence of microbes to the implants by pre-coating the implants with antimicrobials before insertion. Our future studies will address the feasibility of GE-np coated implants to prevent biofilm formation.

Supplementary Material

Refer to Web version on PubMed Central for supplementary material.

Acknowledgements:

We thank Dr. Vera DesMarais and Ms. Hillary Guzik of Analytical Imaging Facility, A.E.C.O.M for training with the use of Leica SP5 confocal microscope and Volocity software. The SP5 confocal microscope is supported by the NCI Cancer Centre grant P30CA013330. We also thank Prof. Uri Samuni and Dr. Jorge Ramos (Queens College-CUNY) for assisting with zeta potential measurements.

Funding sources:

This work was supported by National Institutes of Health grant [P01 HL110900-04].

References:

1. Lebeaux D, Ghigo JM, Beloin C. Biofilm-related infections: bridging the gap between clinical management and fundamental aspects of recalcitrance toward antibiotics. Microbiol Mol Biol Rev 2014;78:510–543. [PubMed: 25184564]
2. Chandra J, Kuhn DM, Mukherjee PK, Hoyer LL, McCormick T, Ghannoum MA. Biofilm formation by the fungal pathogen Candida albicans: development, architecture, and drug resistance. J Bacteriol 2001;183:5385–5394. [PubMed: 11514524]
3. Mirza YH, Tansey R, Sukeik M, Shaath M, Haddad FS. Biofilm and the Role of Antibiotics in the Treatment of Periprosthetic Hip and Knee Joint Infections. Open Orthop J 2016;10:636–645. [PubMed: 28484579]
4. Vinh DC, Embil JM. Device-related infections: a review. J Long Term Eff Med Implants 2005;15:467–488. [PubMed: 16218897]
5. Campoccia D, Montanaro L, Arciola CR. The significance of infection related to orthopedic devices and issues of antibiotic resistance. Biomaterials 2006;27:2331–2339. [PubMed: 16364434]
6. Buommino E, Scognamiglio M, Donnarumma G, Fiorentino A, D'Abrosca B. Recent advances in natural product-based anti-biofilm approaches to control infections. Mini Rev Med Chem 2014;14:1169–1182. [PubMed: 25553429]

7. Galdiero S, Falanga A, Berisio R, Grieco P, Morelli G, Galdiero M. Antimicrobial peptides as an opportunity against bacterial diseases. Curr Med Chem 2015;22:1665–1677. [PubMed: 25760092]
8. Sharifi-Rad J, Sureda A, Tenore GC, et al. Biological Activities of Essential Oils: From Plant Chemoecology to Traditional Healing Systems. Molecules 2017;22.
9. Wang J, Vermerris W. Antimicrobial Nanomaterials Derived from Natural Products-A Review. Materials (Basel) 2016;9.
10. Ankri S, Mirelman D. Antimicrobial properties of allicin from garlic. Microbes Infect 1999;1:125–129. [PubMed: 10594976]
11. Iciek M, Kwiecien I, Wlodek L. Biological properties of garlic and garlic-derived organosulfur compounds. Environ Mol Mutagen 2009;50:247–265. [PubMed: 19253339]
12. Li WR, Shi QS, Liang Q, Huang XM, Chen YB. Antifungal effect and mechanism of garlic oil on Penicillium funiculosum. Appl Microbiol Biotechnol 2014;98:8337–8346. [PubMed: 25012787]
13. Privett BJ, Broadnax AD, Bauman SJ, Riccio DA, Schoenfisch MH. Examination of bacterial resistance to exogenous nitric oxide. Nitric Oxide 2012;26:169–173. [PubMed: 22349019]
14. Li WR, Shi QS, Dai HQ, et al. Antifungal activity, kinetics and molecular mechanism of action of garlic oil against Candida albicans. Sci Rep 2016;6:22805. [PubMed: 26948845]
15. Prager-Khoutorsky M, Goncharov I, Rabinkov A, Mirelman D, Geiger B, Bershadsky AD. Allicin inhibits cell polarization, migration and division via its direct effect on microtubules. Cell Motil Cytoskeleton 2007;64:321–337. [PubMed: 17323373]
16. Ankri S, Miron T, Rabinkov A, Wilchek M, Mirelman D. Allicin from garlic strongly inhibits cysteine proteinases and cytopathic effects of Entamoeba histolytica. Antimicrob Agents Chemother 1997;41:2286–2288. [PubMed: 9333064]
17. Rabinkov A, Miron T, Konstantinovski L, Wilchek M, Mirelman D, Weiner L. The mode of action of allicin: trapping of radicals and interaction with thiol containing proteins. Biochim Biophys Acta 1998;1379:233–244. [PubMed: 9528659]
18. Gordon CA, Hodges NA, Marriott C. Antibiotic interaction and diffusion through alginate and exopolysaccharide of cystic fibrosis-derived Pseudomonas aeruginosa. J Antimicrob Chemother 1988;22:667–674. [PubMed: 3145268]
19. Kumon H, Tomochika K, Matunaga T, Ogawa M, Ohmori H. A sandwich cup method for the penetration assay of antimicrobial agents through Pseudomonas exopolysaccharides. Microbiol Immunol 1994;38:615–619. [PubMed: 7799834]
20. Nichols WW, Dorrington SM, Slack MP, Walmsley HL. Inhibition of tobramycin diffusion by binding to alginate. Antimicrob Agents Chemother 1988;32:518–523. [PubMed: 3132093]
21. Brinker CJ, Keefer KD, Schaefer DW, Ashley CS. Sol-gel transition in simple silicates. J. Non-Crystalline solids 1982;48:47–64.
22. Jurcisek JA, Dickson AC, Bruggeman ME, Bakaletz LO. In vitro biofilm formation in an 8-well chamber slide. J Vis Exp 2011.
23. Zago CE, Silva S, Sanita PV, et al. Dynamics of biofilm formation and the interaction between Candida albicans and methicillin-susceptible (MSSA) and -resistant Staphylococcus aureus (MRSA). PLoS One 2015;10:e0123206. [PubMed: 25875834]
24. Johnson MB, Criss AK. Fluorescence microscopy methods for determining the viability of bacteria in association with mammalian cells. J Vis Exp 2013.
25. Flemming HC, Wingender J, Szewzyk U, Steinberg P, Rice SA, Kjelleberg S. Biofilms: an emergent form of bacterial life. Nat Rev Microbiol 2016;14:563–575. [PubMed: 27510863]
26. Hiramatsu K, Cui L, Kuroda M, Ito T. The emergence and evolution of methicillin-resistant Staphylococcus aureus. Trends Microbiol 2001;9:486–493. [PubMed: 11597450]
27. Kluytmans-Vandenbergh MF, Kluytmans JA. Community-acquired methicillin-resistant Staphylococcus aureus: current perspectives. Clin Microbiol Infect 2006;12 Suppl 1:9–15. [PubMed: 16445719]
28. Cosgrove SE. The relationship between antimicrobial resistance and patient outcomes: mortality, length of hospital stay, and health care costs. Clin Infect Dis 2006;42 Suppl 2:S82–89. [PubMed: 16355321]

29. Dasenbrook EC, Checkley W, Merlo CA, Konstan MW, Lechtzin N, Boyle MP. Association between respiratory tract methicillin-resistant Staphylococcus aureus and survival in cystic fibrosis. Jama 2010;303:2386–2392. [PubMed: 20551409]

30. Metcalf DG, Bowler PG. Biofilm delays wound healing: A review of the evidence. Burns Trauma 2013;1:5–12. [PubMed: 27574616]

31. Burmolle M, Thomsen TR, Fazli M, et al. Biofilms in chronic infections - a matter of opportunity - monospecies biofilms in multispecies infections. FEMS Immunol Med Microbiol 2010;59:324–336. [PubMed: 20602635]

32. Brady RA, Leid JG, Calhoun JH, Costerton JW, Shirtliff ME. Osteomyelitis and the role of biofilms in chronic infection. FEMS Immunol Med Microbiol 2008;52:13–22. [PubMed: 18081847]

33. Ferguson BJ, Stolz DB. Demonstration of biofilm in human bacterial chronic rhinosinusitis. Am J Rhinol 2005;19:452–457. [PubMed: 16270598]

34. Croissant JG, Fatieiev Y, Khashab NM. Degradability and Clearance of Silicon, Organosilica, Silsesquioxane, Silica Mixed Oxide, and Mesoporous Silica nanoparticles. Adv Mater 2017;29:1–51.

35. Jugdaohsingh R Silicon and bone health. J Nutr Health Aging 2007;11:99–110. [PubMed: 17435952]

36. Fujisawa H, Suma K, Origuchi K, Kumagai H, Seki T, Ariga T. Biological and chemical stability of garlic-derived allicin. J Agric Food Chem 2008;56:4229–4235. [PubMed: 18489116]

37. Gupta H, Aqil M, Khar RK, Ali A, Bhatnagar A, Mittal G. Sparfloxacin-loaded PLGA nanoparticles for sustained ocular drug delivery. Nanomedicine 2010;6:324–333. [PubMed: 19857606]

38. Alvarez-Paino M, Munoz-Bonilla A, Fernandez-Garcia M. Antimicrobial Polymers in the Nano-World. Nanomaterials (Basel) 2017;7.

39. Cerca N, Martins S, Cerca F, et al. Comparative assessment of antibiotic susceptibility of coagulase-negative staphylococci in biofilm versus planktonic culture as assessed by bacterial enumeration or rapid XTT colorimetry. J Antimicrob Chemother 2005;56:331–336. [PubMed: 15980094]

40. Sritharadol R, Hamada M, Kimura S, Ishii Y, Srichana T, Tateda K. Mupirocin at subinhibitory concentrations induces biofilm formation in Staphylococcus aureus. Microb Drug Resist 2018;24:1249–58. [PubMed: 29653478]

41. Miller KP, Wang L, Benicewicz BC, Decho AW. Inorganic nanoparticles engineered to attack bacteria. Chem Soc Rev 2015;44:7787–7807. [PubMed: 26190826]

42. Ikuma K, Decho AW, Lau BL. When nanoparticles meet biofilms-interactions guiding the environmental fate and accumulation of nanoparticles. Front Microbiol 2015;6:591. [PubMed: 26136732]

43. Nevius BA, Chen YP, Ferry JL, Decho AW. Surface-functionalization effects on uptake of fluorescent polystyrene nanoparticles by model biofilms. Ecotoxicology 2012;21:2205–2213. [PubMed: 22806556]

44. Wang LS, Gupta A, Rotello VM. Nanomaterials for the Treatment of Bacterial Biofilms. ACS Infect Dis 2016;2:3–4. [PubMed: 27622944]

45. Peulen TO, Wilkinson KJ. Diffusion of nanoparticles in a biofilm. Environ Sci Technol 2011;45:3367–3373. [PubMed: 21434601]

46. Friedman AJ, Han G, Navati MS, et al. Sustained release nitric oxide releasing nanoparticles: characterization of a novel delivery platform based on nitrite containing hydrogel/glass composites. Nitric Oxide 2008;19:12–20. [PubMed: 18457680]

47. Austin TO, Matamoros AJ, Friedman JM, et al. Nanoparticle Delivery of Fidgetin siRNA as a Microtubule-based Therapy to Augment Nerve Regeneration. Sci Rep 2017;7:9675. [PubMed: 28852085]

48. Nacharaju P, Tuckman-Vernon C, Maier KE, et al. A nanoparticle delivery vehicle for S-nitroso-N-acetyl cysteine: sustained vascular response. Nitric Oxide 2012;27:150–160. [PubMed: 22705913]

49. Lu X, Samuelson DR, Rasco BA, Konkel ME. Antimicrobial effect of diallyl sulphide on Campylobacter jejuni biofilms. J Antimicrob Chemother 2012;67:1915–1926. [PubMed: 22550133]

50. Ranjbar-Omid M, Arzanlou M, Amani M, Shokri Al-Hashem SK, Amir Mozafari N, Peeri Doghaheh H. Allicin from garlic inhibits the biofilm formation and urease activity of Proteus mirabilis in vitro. FEMS Microbiol Lett 2015;362.

51. Cruz-Villalon G, Perez-Giraldo C. Effect of allicin on the production of polysaccharide intercellular adhesin in Staphylococcus epidermidis. J Appl Microbiol 2011;110:723–728. [PubMed: 21205098]

52. Lihua L, Jianhuit W, Jialini Y, Yayin L, Guanxin L. Effects of allicin on the formation of Pseudomonas aeruginosa biofinm and the production of quorum-sensing controlled virulence factors. Pol J Microbiol 2013;62:243–251. [PubMed: 24459829]

53. Jakobsen TH, van Gennip M, Phipps RK, et al. Ajoene, a sulfur-rich molecule from garlic, inhibits genes controlled by quorum sensing. Antimicrob Agents Chemother 2012;56:2314–2325. [PubMed: 22314537]

54. Jakobsen TH, Warming AN, Vejborg RM, et al. A broad range quorum sensing inhibitor working through sRNA inhibition. Sci Rep 2017;7:9857. [PubMed: 28851971]

55. Deva AK, Adams WP, Jr., Vickery K. The role of bacterial biofilms in device-associated infection. Plast Reconstr Surg 2013;132:1319–1328. [PubMed: 23924649]

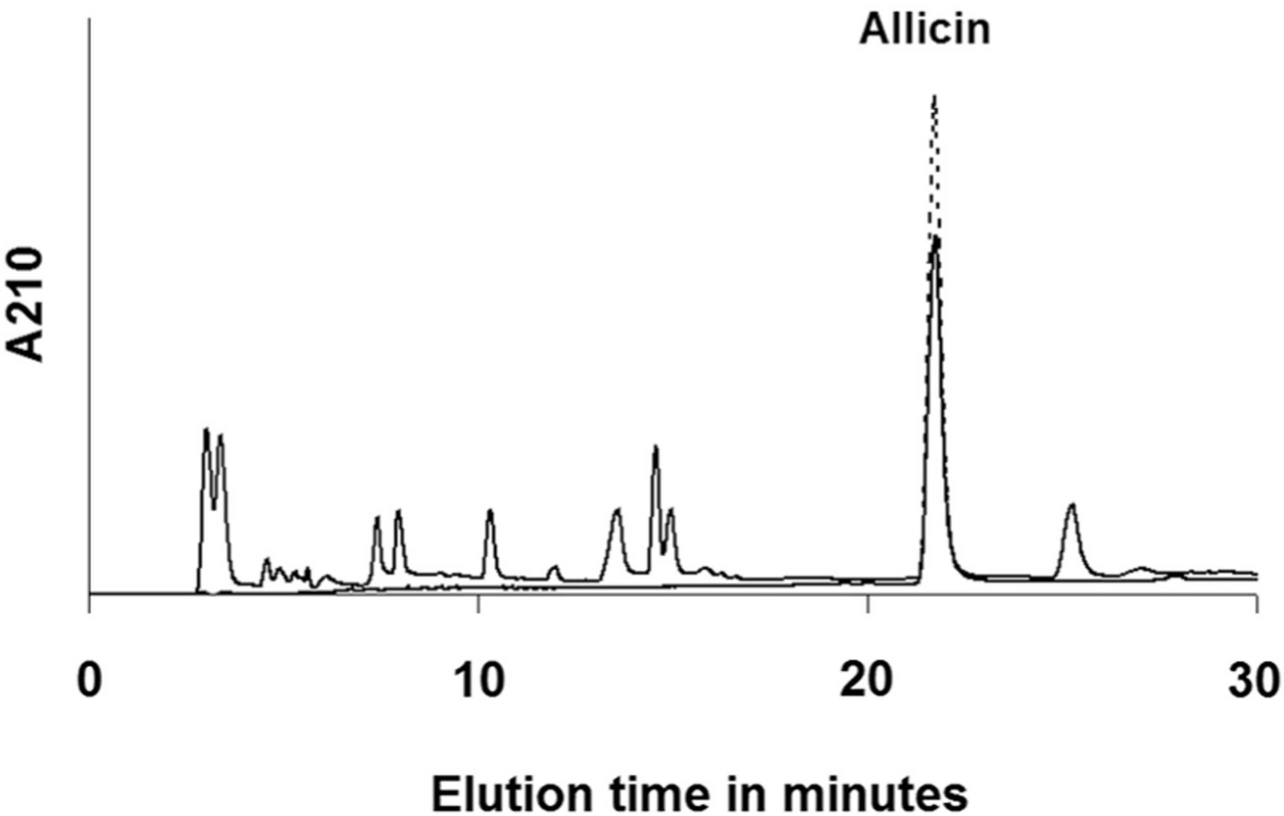

Figure 1.

RP-HPLC chromatogram of the garlic extract The garlic extract (solid line) and allicin standard (broken line) were analyzed on a c18 column as described in the methodology section of supplementary material. The allicin pure standard peak overlapped with the major peak in the garlic extract.

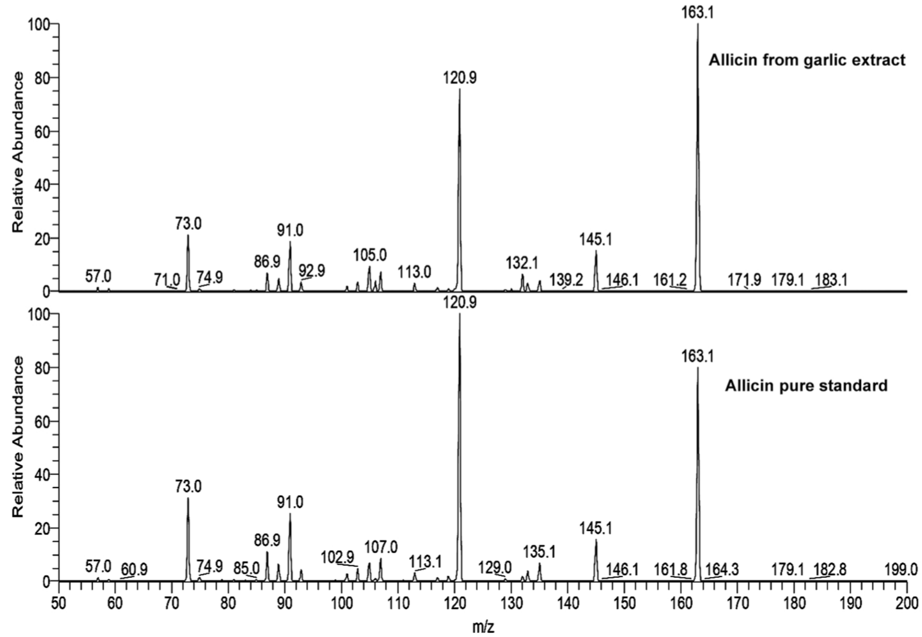

Figure 2.

Comparison of MS/MS analysis of m/z 163 from allicin from the garlic extract (top) and pure standard (bottom).

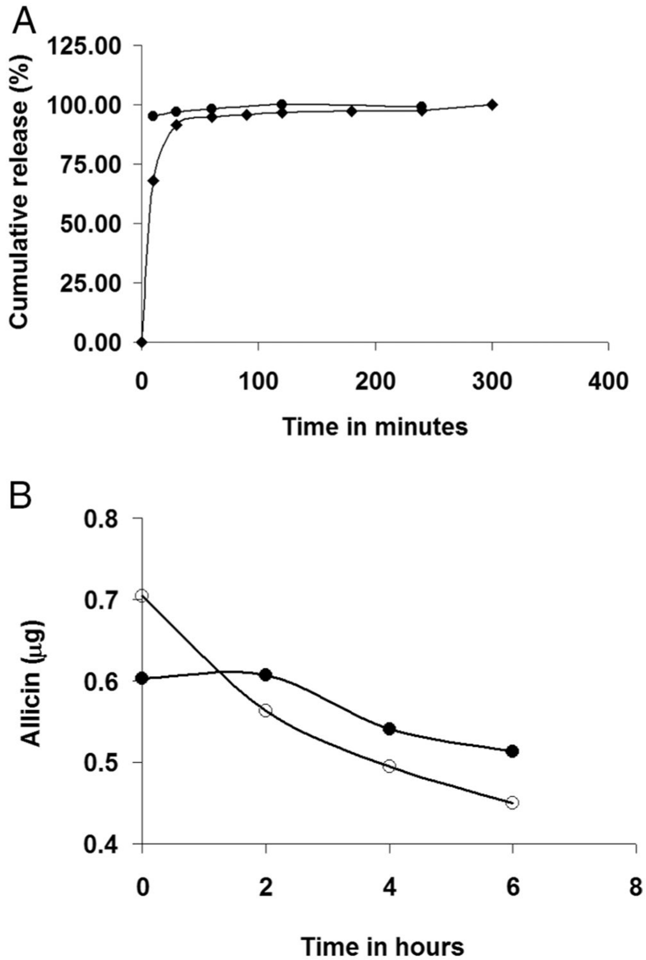

Figure 3.

(A) Rate of release of garlic extract components from GE-np-control (circle) and GE-np (diamond). The release of total garlic extract from the particles into PBS at room temperature was monitored at 210 nm. **(B)** Stability of allicin at 37°C. The amount of allicin present in garlic extract (open circle) and also in the extract released from GE-np (closed circle) at 37°C was monitored by RP-HPLC. The initial concentration of garlic extract matched with the total amount of extract released from GE-np. Due to the slow release of extract from the GE-np, the initial concentration of allicin was lower for GE-np as compared to the extract. However, allicin in the garlic extract was more rapidly degraded as compared to that in GE-np.

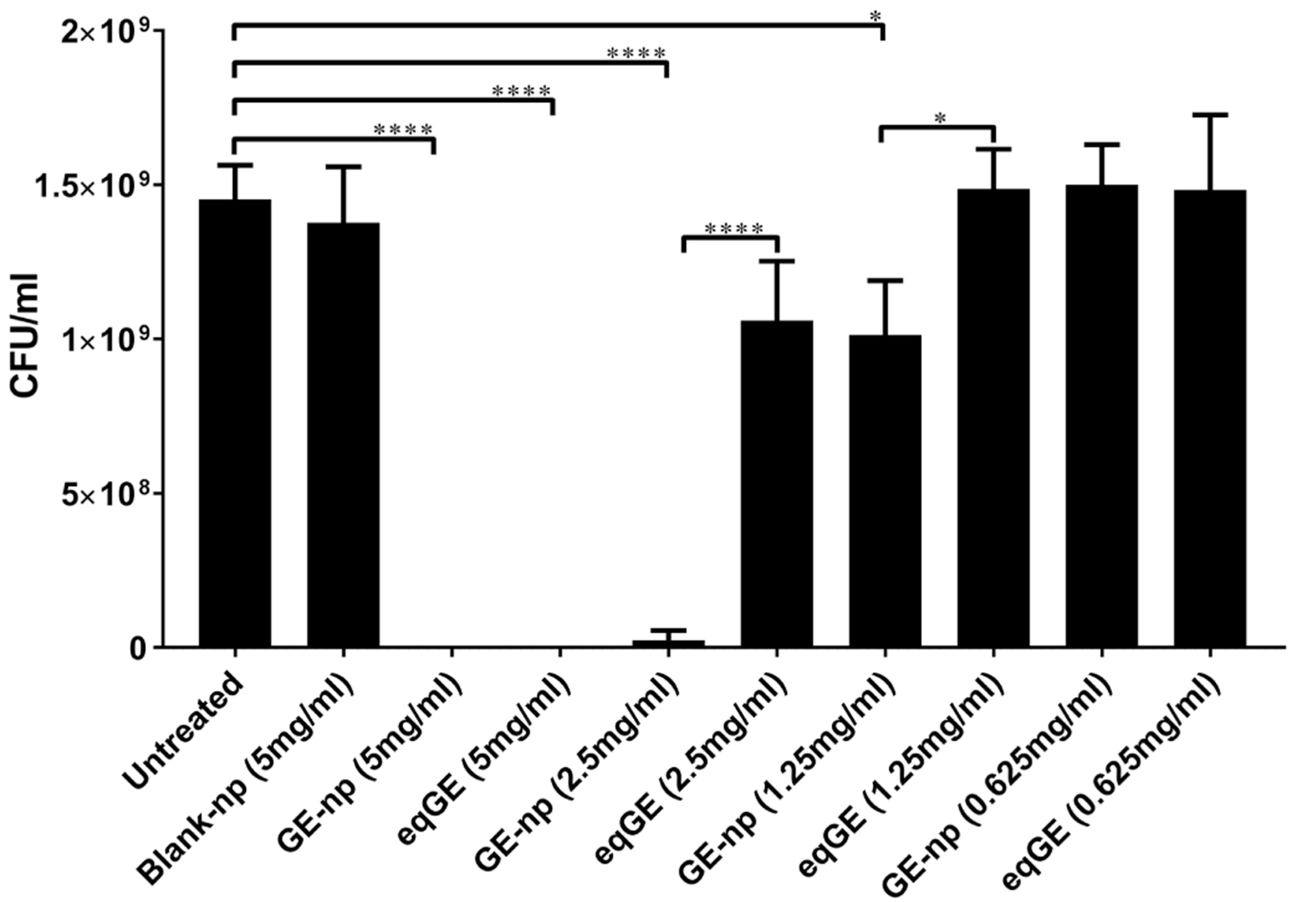

Figure 4.

Antibacterial effects of GE-np. Susceptibility of planktonic form of MRSA to varying concentrations of GE-np (0.625, 1.25, 2.5 and 5 mg/ml) was determined by CFU counts. For each concentration of GE-np, equivalent concentration of garlic extract (eqGE) was taken as control. The data is represented as the mean of three independent experiments ± standard deviation. Statistically significant inhibition as compared with untreated control was denoted by p-values (*$p \leq 0.05$, ****$p \leq 0.0001$) calculated by one-way ANOVA.

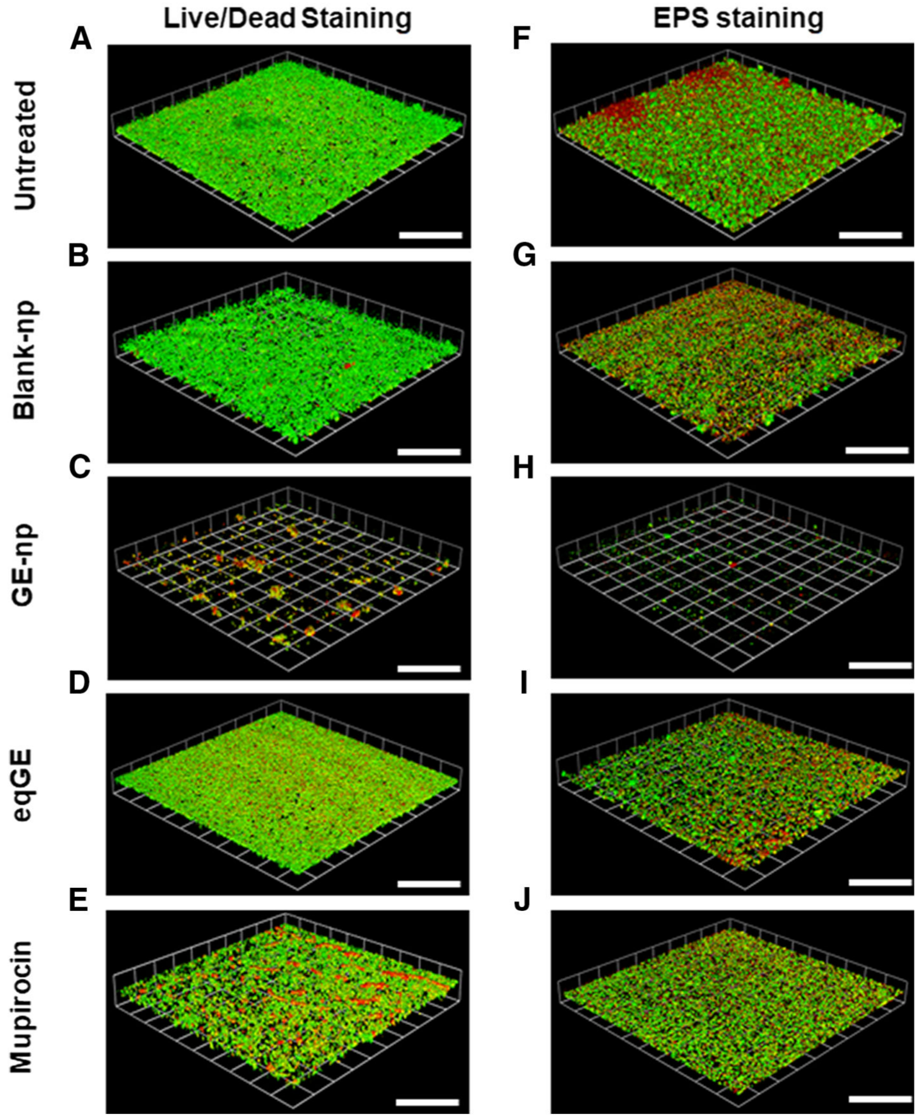

Figure 5.

Anti-biofilm effects of GE-np. Representative 3D-images of 48-hour old MRSA biofilms grown in an 8-well chamber slide treated with (**A, F**) media alone (untreated), (**B, G**) 5mg/ml blank nanoparticles, (**C, H**) 5 mg/ml GE-np, (**D, I**) equivalent garlic extract or (**E, J**) mupirocin (1 mg/ml). Concurrent overlay of two different staining procedures separately, permit the visualization of bacterial viability [live (green) and dead (red/yellow)] (**A, B, C, D, E**) and extra polymeric substances (EPS) [polysaccharides (green) and proteins (red)] (**F, G, H, I, J**). The images were acquired using Leica SP5 confocal laser scanning microscope. The 3D-images were constructed using Volocity software v6.3. The scale bars represent 100 μm for all images. The confocal experiments were performed twice.

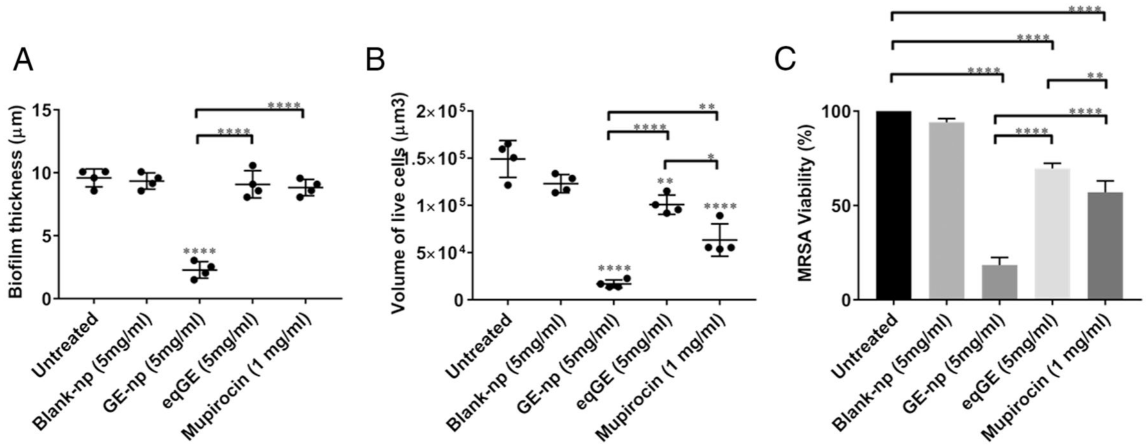

Figure 6.

Quantitative analysis of biofilm architecture **(A)** Biofilm thickness and **(B)** Biofilm volume. The thickness and volume of viable cells in the biofilms exposed to GE-np, blank-np, equivalent garlic extract (eqGE) or mupirocin were observed in the z-stack construction of the confocal images and was quantified using Volocity software v6.3. The differences were examined and compared with that of the untreated biofilms (media alone). The results represented as mean ± SD, were from multiple images of two independent confocal experiments. Statistical significance (*$p \leq 0.05$, **$p < 0.01$, ****$p < 0.0001$) was determined by one-way ANOVA. **(C)** Biofilm viability. The percentage viability of biofilm-associated cells was evaluated using XTT assay. The results are represented as mean ± SD from three independent experiments performed in triplicates. Statistical significance (**$p < 0.01$, ****$p < 0.0001$) was determined by one-way ANOVA.

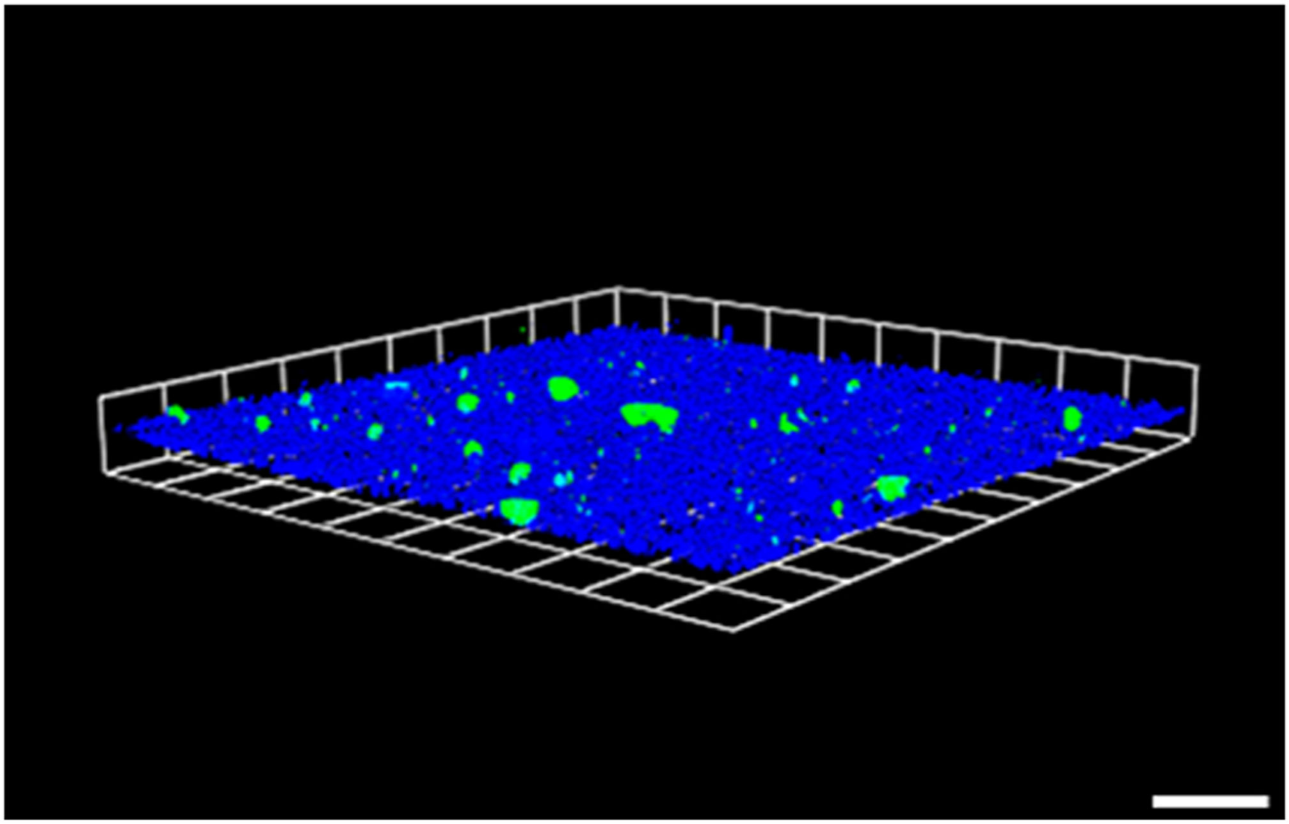

Figure 7.
Nanoparticles adhere and penetrate through the mature biofilm. Representative 3D-image of 48-hour old MRSA biofilm (blue) grown in an 8-well chamber slide treated with 0.5 mg/ml blank-np (green). The polysaccharide component of EPS was stained with concanavalin A-405. The images were acquired using Leica SP5 confocal laser scanning microscope and the image was constructed using Volocity software v6.3. The scale bars represent 100 μm. The experiment was performed twice.